Coping with copepods:
Do right whales (*Eubalaena glacialis*) forage visually in dark waters?

Thomas W. Cronin[1]
Jeffry I. Fasick[2]
Lorian E. Schweikert[3]
Sönke Johnsen[4]
Lorren J. Kezmoh[1]
Mark F. Baumgartner[5]

[1]Department of Biological Sciences, University of Maryland Baltimore County, Baltimore, MD 21250 USA
[2]Department of Biological Sciences, The University of Tampa, Tampa, FL 33606, USA
[3]Department of Biological Sciences, Florida Institute of Technology, Melbourne, FL 33606, USA
[4]Biology Department, Duke University, Durham, NC 27708 USA
[5]Biology Department, Woods Hole Oceanographic Institution, Woods Hole, MA 02543 USA

Keywords:
right whale, visual sensitivity, contrast vision, environmental radiometry

Author for correspondence:
Thomas W. Cronin
email: cronin@umbc.edu

Abstract

North Atlantic right whales (*Eubalaena glacialis*) feed during the spring and early summer in marine waters off the northeast coast of North America. Their food primarily consists of planktonic copepods, *Calanus finmarchicus*, which they consume in large numbers by ram filter feeding. The coastal waters where these whales forage are turbid, but they successfully locate copepod swarms during the day at depths exceeding 100 m, where light is very dim and copepod patches may be difficult to see. Using models of *E. glacialis* visual sensitivity together with measurements of light in waters near Cape Cod where they feed and of light attenuation by living copepods in seawater, we evaluated the potential for visual foraging by these whales. Our results suggest that vision may be useful for finding copepod patches, particularly if *E. glacialis* searches overhead for silhouetted masses or layers of copepods. This should permit the whales to locate *C. finmarchicus* visually throughout most daylight hours at depths throughout their foraging range. Looking laterally, the whales might also be able to see copepod patches at short range near the surface.

1. Introduction

North Atlantic right whales (*Eubalaena glacialis*) rank among the most impressive animals on earth, reaching lengths exceeding 18 m and masses near 100,000 kg. The three species of right whales, along with the bowhead whale, are assigned to the family Balaenidae, possibly the earliest-branching taxon of the Cetacea [1]. Unlike other baleen whales (mysticetes), whose predatory behaviors include lunges (e.g. [2]) and sometimes the use of bubble nets to corral prey [3], right whales use their forward motion to ram filter feed [4]. They open their mouths to form a large and sophisticated whale-powered plankton net, swimming forward and filtering out

zooplankton from seawater exiting the mouth through their baleen plates. When at the surface, this is called “skim feeding”.

Such feeding demands significant energy, which limits speed and thus the choice of prey to creatures that cannot easily evade the approaching whale [4]. *E. glacialis* specializes on small crustaceans, primarily the copepod *Calanus finmarchicus*. The whales’ energetic demands require that they filter copepod patches of unusually high density in the highly productive waters in the northwestern Atlantic Ocean during their springtime residence [5]. *E. glacialis* unfailingly locates these [6] and can track the vertical migrations of its prey, often feeding at depths exceeding 100 m [5,7]. Diving is energetically costly and time-limited, so the whales must consistently locate prey just to recover the cost of the dive itself. If copepod distributions permit it, they conserve energy by feeding at or near the surface. Finding food probably involves both knowing how local oceanographic and hydrographic features concentrate copepod stocks and using specialized sensory systems to locate smaller-scale patches that contain the highest copepod densities (reviewed in [4]).

Right whales apparently earned their common name by being the “right whales” for early whalers to hunt. They forage at slow speeds near coasts, often on the surface, and their bodies are rich in baleen and blubber. The same characteristics that placed them at the mercy of whalers endanger them from modern threats, especially in northwestern Atlantic waters. They live in some of the most active sea lanes in North America, they feed in shallow waters where boat traffic is heavy, and they feed where fixed fishing gear is abundant. Together with their tendency to linger on the surface and their limited swimming speeds, this puts them at constant risk of injury or death from ship strikes, collision with smaller boats, and entanglement in fishing

gear. Such frequent interactions with humans and their numerous environmental impacts encouraged its researchers to dub *E. glacialis* "the urban whale" [8].

Unlike toothed whales, mysticetes do not echolocate (see [9]), but some species use vision to locate prey [2]. We thus set out to learn whether *E. glacialis* could sight concentrations of *C. finmarchicus* at the depths at which they feed. To do this, we needed to know the visual sensitivity of the whales, the light available at feeding depths, and the visual contrast of copepod patches against the background light.

Like most mysticetes, balaenids are rod monochromats [10-14]. Otherwise, their eyes are of typical mammalian design, resembling somewhat enlarged bovine eyes. Expression analysis of *E. glacialis* rod visual pigment places its peak wavelength of absorption at 493 nm [15,16], rather short for a coastal species [15,17]. Combining the visual pigment data with eye measurements available from other balaenids, we estimated the absolute spectral sensitivity of *E. glacialis*. Together with measurements of spectral attenuation by live *C. finmarchicus* and of the photic properties of water in locations where *E. glacialis* feeds, we evaluated the potential for the whales to sight copepod concentrations at feeding depths. Our results suggest that vision may indeed be used by these animals to find prey, particularly if they locate copepod aggregations by looking upwards.

2. Materials and Methods

(a) Estimation of visual spectral sensitivity

We used Land's [18,19] equation for sensitivity, which requires pupil diameter, lens focal length, photoreceptor (rod outer segment) diameter and length, and the rod visual pigment absolute absorbance spectrum. Of these, only the visual pigment's relative absorbance spectrum is known

for *E. glacialis* [16], and no eyes sufficiently well preserved for dimensional measurements were available. However, published data from the related and similarly-sized balaenids *E. australis* (southern right whale) and *B. mysticetus* (bowhead whale) [14,20,21] provide reasonable estimates for the ocular properties of *E. glacialis*. The methods used to estimate these measurements and associated data are described in the supplementary materials.

(b) Copepod spectral absorption and contrast

Live copepods, predominantly the 5th copepodite stage of *C. finmarchicus*, were gently collected with plankton nets in the Great South Channel, a springtime right whale habitat, kept chilled, and shipped to Baltimore for measurements of spectral attenuation. The attenuations over a range of copepod concentrations were analyzed in a cylindrical spectrophotometer cell 10 cm in length. Further details are available in supplementary materials.

(c) Radiometric measurements in the field

Underwater spectral radiometry was done from the research vessels R/V *Tioga* and the NOAA Ship *Gordon Gunter*. At each station, three replicate casts were made with a free-falling Profiler II instrument (Satlantic, Halifax, Novia Scotia) equipped to measure spectral profiles of downwelling irradiance and horizontal radiance (348-802 nm at ~3-nm intervals). Measurements were averaged into 4-m-deep bins beginning at the surface (giving averages at depths of 2 m, 6 m, 10 m, etc). Four series at separate locations within right whale foraging habitats obtained measurements either to the bottom or to depths where readings were indistinguishable from the electronic noise of the instruments (typically ~ 40 to 70 m).

Two series were completed on April 4, 2012, at locations in Wilkinson Basin (42 23N,69 86W; solar elevation ~47°) and near the entrance to Cape Cod Bay (42 07N,70 27W; solar elevation ~23°). Two additional series were completed in May 2013, both in the Great South Channel southeast of Cape Cod (May 8: 41 15N, 69 18W; solar elevation ~58°; May 9: 41 19N, 69 19W; solar elevation ~30.5°). Measurements occurred on afternoons (~12:00 to ~17:00 local time) of days that were clear (2012) to overcast or with thin cloud cover (2013). All readings were interpolated into 1-nm intervals, 350 to 800 nm, and converted to photon fluxes for further use. Since the Satlantic instruments were not configured to measure downward radiance, we also used an earlier data set from a site near Cape Cod Bay off the coast of New Hampshire [22]. In that study, conducted at noon on June 30, 2000, downward radiance and horizontal radiance towards and away from the solar direction were computed at 5-m intervals.

3. Results and Discussion

(a) Estimation of visual spectral sensitivity

The optical sensitivity (S) of receptors in an eye in photon units (n photons absorbed per receptor at a given radiance R, or n/R) can be found using the equation [18,19]:

$$(1) \qquad S(\lambda) = \frac{\pi}{4} D^2 \Delta\rho^2 P_{abs}(\lambda) \ .$$

Here, λ is wavelength, D is pupil diameter, $\Delta\rho$ is the photoreceptor acceptance angle (radians), and P_{abs} is the proportion of photons absorbed by a photoreceptor (a function of λ). P_{abs} (absorptance) is calculated from total absorbance, the product of the absorbance per unit length (α) at wavelength λ and photoreceptor length (l). For rod-sized photoreceptors with diameter d in an eye of focal length f, $\Delta\rho^2$ is $(d/f)^2$ in steradians (sr), so S is described in units of photons

absorbed multiplied by cm^2 and sr. Multiplying this by radiance (photons s^{-1} cm^{-2} nm^{-1} sr^{-1}) gives photons absorbed per rod per second per nm. After substitution, Eq. 1 becomes:

$$(2) \qquad S(\lambda) = 0.62\, D^2\, (d/f)^2\, (1 - 10^{-\alpha(\lambda)l}) \quad .$$

Thus, calculating the optical sensitivity of the *E. glacialis* eye requires pupil diameter, focal length, and photoreceptor length and diameter. No material from *E. glacialis* was available for any of these measurements, so we used light and electron micrographs of *B. mysticetus* (bowhead) rods from [14], from which we estimated rod length to be 30 µm and diameter as 1.4 µm. We used published data from *E. australis* [20] to approximate the optical properties of eyes of *E. glacialis*, comparing the results with data from *B. mysticetus* [21] to check their validity (see supplementary material and tables S1 and S2). Using the *E. australis* results and the absorptance spectrum for a 30-µm rod based on an absorbance of 0.015 per µm at the 493-nm peak [23] and a standard visual pigment template for a 493-nm rhodopsin [24], we computed sensitivity at 1-nm intervals from 400 to 700 nm (figure 1). These measures of optical sensitivity do not include light lost during its passage through the ocular media or reflected by the tapetum, which we consider later on.

(b) Copepod light attenuation

If right whales use vision to forage, copepods obviously must be visible to them. Individual *C. finmarchicus* are probably too small to see, but compact, dense copepod patches could form visible regions of contrast against the background radiance. Our attenuation measures (figure S1, raw data, dotted line) were from a 10-cm spectrophotometer cell). For a 1-m path length (in other words, the same numbers of copepods but in a 1-m-long cell), they correspond to attenuations for natural concentrations of 0.1, 0.3, 0.6, and 1.0 per ml (10^5 to 10^6 copepods per

m^3). Natural densities of copepods in locations where *E. glacialis* whales forage range from ~10^4 to 10^6 per cubic meter [5,6**].** A curve was fit to the mean spectral attenuation at the three lowest concentrations, forced to pass through the origin (figure 2, thin solid line). This fitted curve was converted to absorptance, the fraction of light absorbed (figure 2, dashed curve).

The Weber contrast of a copepod patch against the unobstructed background radiance is

(3) $C = |N_b - N_p|/N_b$,

where N_b is number of photons detected by retinal photoreceptors from the background radiance, and N_p is the number of photons detected from light at the location of the copepod patch. (Weber contrast usually takes both positive and negative values, but we used absolute Weber contrast here because minimum contrast sensitivity concerns only the level, not the sign, of the contrast.) Both *N* values vary with the numbers of receptors involved per unit "pixel" of the scene and their integration times, and of course with the actual spectra and radiances viewed. At zero range, for basically flat attenuation spectra like those through patches of copepods (figure S1) and considering only attenuation, *C* is equal to patch absorptance (i.e. C ~ 1 – N_p/N_b, figure 2). Minimum contrast sensitivities (contrast thresholds) for visual systems across animals range from 0.01 to 0.05 [25], where the lower limit is probably set by photoreceptor and neural noise. Critically, there must also be enough light available to make detection of such a contrast statistically possible [18,19]. Light measurements in *E. glacialis* foraging habitats provided the data needed to compute photon detection rates and contrasts.

(c) Radiometric measurements in the field and *E. glacialis* photon detection rates

Peak primary production in the ocean near Cape Cod occurs during the late winter and early spring. Whales arrive a month or two later, when the copepod prey are well fed and often

diapausing at depths of hundreds of meters [4]. Depth profiles of downwelling irradiance collected in *E. glacialis* feeding habitats were used to calculate diffuse attenuation coefficients, to characterize the waters there. Figure 3*a* shows these for the most turbid water (Wilkinson Basin, April 4, 2012) and the clearest water (Great South Channel, May 8, 2013) we encountered (figure 3*a* also shows attenuation coefficients from [22] discussed later). Waters where right whales forage are typical of coastal regions [26], with elevated light attenuation and peak transmission of green/yellow light (figure 3). Such conditions restrict visual foraging, not only because light levels are low, but also because these waters contain plankton and other suspended solids. Seeing through such water can be challenging. Horizontal radiance profiles for the Wilkinson Basin (figure 3*b*) and the Great South Channel series (figure 3*c*) are dominated by spectrally narrow, green/yellow light. Waters like these seem ill-suited for visual foraging far below the surface, particularly since the spectral sensitivity of *E. glacialis* is poorly matched to the light it views at depths below just a few meters (compare figures 1 and 3).

For a North Atlantic right whale viewing a scene horizontally over the depth ranges where we measured horizontal radiance, the rate of photon capture is simply the product of the rod's sensitivity (figure 1) and the radiance at that depth, summed over the full sensitivity spectrum of the visual pigment in the retina (here we used 400 to 700 nm, since it encompassed essentially the full range of available light). Photon capture rates must be corrected for the integration time of a rod. When dark-adapted, rods have long integration times, approaching 2 s in some ectothermic vertebrates [25,27,28], but mammalian rod integration times are certainly shorter. We used 1-s integration times in our calculations (note that photon radiances were also measured per second). We then corrected for transmission loss through the eye (80% transmission, [29]) and the quantum efficiency for rhodopsin (0.69, [30]) to get actual photon

detections per rod per one-second integration time. However, we ignored tapetal reflection. Mysticete whales have well-developed and extensive tapeta [31,32], which reflect significant quantities of photons back through the retina. Potentially, this could increase photon absorption by 50% or more, but without actual measurements, we decided to ignore this effect.

In the coastal waters off Cape Cod, photon detection rates decrease rapidly with depth (figure S2). Average rates reach one photon per second per rod at depths as shallow as ~35 m in Wilkinson Basin. While the photon detection rates we calculated depend on a number of assumptions, their rapid decrease with depth means that moderate errors in our assumptions (e.g., rod integration times, tapetal effects) have relatively minor effects on the outcomes of our calculations.

(d) Contrast vision and visual foraging by *E. glacialis*

We can now evaluate contrast vision. Due to the statistics of the arrival rates of photons at single receptors, the minimum possible detectable Weber contrast (C_{min}) of a visual object against background is equal to 2.77 over the square root of the average number of photons detected in one integration time (N) of the photoreceptors involved [29]:

$$(4)\quad C_{min} = 2.77/\sqrt{N}\ .$$

Using photon detection rates (figure S2), we computed minimum discriminable contrast vs. depth. Figure 4 shows results for sites with the lowest rates (Wilkinson Basin) and the greatest ones (Great South Channel). In horizontal radiance, rod photon capture rates sufficient to support a conservative mammalian contrast threshold (0.05) exist only down to ~12 m in Wilkinson Basin (figure 4a) and ~30 m in the Great South Channel (figure 4b). But rods do not act alone; in mammalian retinas commonly 1000 or more rods summate onto a single luminance-

detecting retinal ganglion cell (RGC) [28,29,33]. Cetaceans in particular have exceptionally large RGCs called “giant retinal ganglion cells” which probably acquire input from many rods [31,32]. Rod convergence ratios have never been directly measured in cetaceans, but RGC densities and distributions are known for many cetacean retinas [31,32] (in particular for two mysticetes, the minke whale [34] and the gray whale [35]), and rod densities are available for a few toothed whale species [12]. Like other cetaceans [31], minke and gray whales have two areas of elevated RGC density, in the temporal and nasal retinas (sampling forward-looking and lateral vision respectively) [34,35]. Calculated rod:RGC ratios imply that many, many rods converge onto single RGCs in these whales, even in their regions of best vision. The current mammalian champion for convergence ratios is the highly nocturnal owl monkey, where between 800 and 10,000 rods converge per RGC, varying with retinal region [36]. Data from [12,34,35] suggest that mysticete whales reach similar ratios, approaching 2,000:1 area centralis regions in the temporal and nasal retina and perhaps 8,000:1 in the periphery. These levels of summation limit spatial resolution, but might permit whales to see dim, fuzzy, low-contrast objects like plankton clouds well below the surface during the day.

Based on summations of 100 or 1000 rods, we recalculated contrast:depth relationships for right whale vision (figure 4). When 100 rod signals are summed, whales potentially could sight objects with contrast of 0.05 down to ~45 m depth even in the gloomy photic conditions of Wilkinson Basin (figure 4*a*) and to ~70 m in the Great South Channel (figure 4*b)*. Summing 1000 rods per RGC extends these depths to ~55 and ~90 m, respectively. These are still well above the deepest foraging depths, which can exceed 150 m [5]. Given these results, is visual foraging likely over much of the whales’ springtime feeding depth range in the western Gulf of Maine?

Unfortunately, we don't know precisely how copepods are distributed on fine spatial scales, nor the geometry of high-density micropatches found within the larger copepod swarms. If copepods are fairly evenly distributed within their preferred depth range during the day, there is little for a right whale to see, since it surely does not image individual plankton, and the overall haze produced by the copepod clouds fills the visual field. Perhaps right whales look for contrasting patches of unusually high local density. If these exist, they are most useful to the whale if they are sufficiently small to spot against the background light passing through the lower-density regions of the swarm. Figure 2 suggests that for a patch thickness of 1 m, Weber contrast is above 0.05 for all copepod concentrations above 10^5 m^{-3}. Such a contrast is only visible at ranges within fractions of a meter – probably not relevant to a whale. At greater distances, the intervening turbidity will quickly introduce veiling light, which will obscure the dim patch behind it.

Another potential problem is that copepods do not just absorb and scatter light coming from behind them. They also scatter downwelling light arriving from the surface, and this laterally scattered light will reduce - and possibly even eliminate – the contrast they produce against the background. The downwelling radiance is so much brighter than the horizontal radiance (figure 5*a*) that even weak scattering in the direction of the whale's eye may obliterate the background contrast. Indeed, brightly scattering patches of plankton could themselves become prominent visual targets [37]. At this point, we don't have the measurements or images to determine just what a patch of copepods looks like underwater at any depth. And as already noted, we lack definitive descriptions of patches of copepods. Based on the results reported here, however, we suggest that visual foraging by whales looking laterally into the water column is likely to be most useful during skim-feeding or at very shallow depths.

This does not rule out visual foraging deeper down. Instead of looking horizontally, right whales could search overhead for copepods using their dorsal visual field. Since forward scattering of light is included in our copepod attenuation measurements, we can reasonably accurately predict the downward light attenuation by any given concentration of copepods if we know patch dimensions. Even if the copepods are randomly dispersed, their lower average concentrations would be offset by the thickness of the horizontal pancake within which they exist, so the whale could visually experience something like a cloud passing in front of the downwelling light – which might be all it needs to localize the copepod mass. Work on zooplankton light absorption and scattering suggests that their visual predators should, in fact, look more laterally near the surface and more vertically at depth [37]. But for this to work for *E. glacialis*, the whale must monitor the overhead visual field, and we do not know if right whales do this.

Looking upwards is advantageous mostly because the downward-directed radiance is far brighter than the horizontal radiance and also because very little veiling light is added in this direction. We thus included data on such radiance collected in June 2000 at a location not far from Cape Cod, 80 km seaward from Portsmouth, New Hampshire [22]. The water quality at this location was similar to that of the Great South Channel in May 2013 (figure 2*a*). Viewing horizontal radiance (either towards or away from the sun) in these photic conditions, whale rods could detect photons with similar depth profiles for the 2000 and 2013 data (compare figure S2 with figure 5*a*, dark solid and dashed lines). In comparison, the much brighter downward radiances produced photon detection rates some two orders of magnitude higher (figure 5*a*, dotted line). Using downward radiance, right whales may be able to spot cubic-meter-size, copepod patches with 100,000 or more copepods at depths of ~140 m by spatially summing 1000

rods (figure 5*b*). (If 8,000 rods summate, a contrast of 0.05 is perceptible down to ~160 m, not shown.) In thick layers of copepods, even if they are randomly distributed, the contrast would nearly always be visible throughout the entire foraging depth range near Cape Cod. Thus, whales could easily detect patches with copepod densities known to occur at their foraging depths, at least in locations of fair water clarity. Densities and distributions of RGCs in ventral retinas of *E. glacialis* should be measured to learn whether this could be done even without postural changes by the whales.

Blue whales sight prey concentrations when swimming upwards, looking ahead and visually targeting patches of krill against surface light for a feeding lunge [2], so overhead monitoring by right whales should not be ruled out. It would be interesting to make depth casts of an upward-looking radiance meter coupled with an optical plankton recorder so that the effects of copepod layers on downwelling light could be monitored directly. It would also be revealing to attach releasable cameras (like the "Crittercams" used with blue whales [38]) to foraging right whales. While the dim illumination could be problematic, it should be possible to monitor whether the whales occasionally roll or lift their heads to search the overhead light field. This could be coupled with recorders of depth, speed, and orientation to reconstruct the dynamics of the whales as they approach foraging depths. Note that right whales need not penetrate the full thickness of a copepod layer to know that they are at the right depth; the dimming of light as they pass into the layer is likely to be a usable signal in itself. Of course, they also must be able to discriminate the quick dimming of light by a passing cloud from that of a copepod layer, which must present a challenge.

Right whales successfully feed even when copepods in a given region vertically migrate, primarily orienting to regions of high densities regardless of whether these occur at the surface or

at depth [7]. These migrations should favor a visual role in predation, because migrating copepods are generally at their deep location during the day, when the brighter light could help to spot them, and move to the upper waters at night, when the whales could skim-feed or perhaps even sight them in surface waters at nocturnal light levels. On the other hand, our measurements were made over a somewhat limited range of weather conditions and solar elevations, and we did not explore the temporal limits of potential visually directed foraging. Whales are likely to be capable of doing this for only part of the day, at least away from surface waters.

Another challenge for right whales is their descent from sunlit surface waters to quite dark depths when they dive to feed. Tracks of diving whales indicate that they reach foraging depths in only a few minutes [5]. To see at all in this new photic environment, they would have to dark-adapt unusually rapidly. Humans require over half an hour for full dark adaptation, longer than the entire dive duration of *E. glacialis*. In comparison, deep-diving elephant seals fully dark-adapt within six minutes, to thresholds well below those of human controls [39], and bottle-nose dolphin pupils fully constrict within 8 seconds (although the relaxation times are not known) [40]. Retinas of *B. mysticetus*, and probably retinas of other (all?) mysticete whales retain the neural pathways used for cone signaling, even in the absence of cone outer segments, implying that rod-mediated vision can flow through the typical bright-light pathway [14]. Perhaps whales maintain separate light-adapted and dark-adaptive networks running in parallel, although such a dual system has not previously been described.

North Atlantic right whales make V-shaped dives when searching for plankton, which implies rapid or continuous dark adaption. These are thought to be used to track prey depths and locations. During subsequent foraging dives, the whales may fully adapt to dim light and become capable of continuously monitoring prey density and its changes in depth as they feed.

(e) Other methods of prey detection

Prey search is surely a multimodal process, perhaps involving a combination of olfactory senses (which are poorly developed in cetaceans, although perhaps not in balaenids [41]), sensory taste buds in the oral cavity (also limited in cetaceans, see [42]), and mechanoreception, where foraging whales may monitor impacts of plankton with bristles on their rostrum or on the tongue itself [4]. Our study supports the notion that whales can use their eyes in prey search, even in turbid and relatively dark environments. Nevertheless, we still have no clear understanding of whether they would search for prey as visible patches (which might be visible looking horizontally not far below the surface), as dim clouds stretching overhead, or in some other way. Equally distressing is that we don't understand how - or if - their vision might be involved in underwater object detection and control of avoidance behavior. Knowing this could be critical for finding ways of reducing entanglements with fishing gear. On the bright side, this work identifies some promising research questions and approaches that could bring us closer to understanding the visual world of North Atlantic right whales.

Acknowledgements. We thank B. Arnold and K. Feller for help with the copepod spectroscopy, S. Laney for the use of the submersible radiometer, A. Greco for assistance with electron microscopy, and L. Peichl for advice and comments on the manuscript.

Funding statement. This work is based on research supported by the Air Force Office of Scientific Research, under grant no. FA9550-12-1-0321. Support for field observations was provided by the Woods Hole Oceanographic Institution and by the National Oceanic and Atmospheric Administration (NOAA) Northeast Fisheries Science Center.

References

1. Gatesy J, Geisler JH, Chang J, Buell C, Berta A, Meredith RW, Springer MS, McGowen MR. 2013 A phylogenetic blueprint for a modern whale. *Mol. Phylogen. Evol.* **66**, 479-506.

2. Goldbogen JA, Calambokidis J, Friedlaender AS, Francis J, DeRuiter SL, Stimpert AK, Falcone E, Southall BL. 2012 Underwater acrobatics by the world's largest predator: 360° rolling manoeuvres by lunge-feeding blue whales. *Biol. Lett.* **9**, 20120986.

3. Wiley D, Ware C, Bocconcelli A, Cholewiak D, Friedlander A, Thompson M, Weinrich M. 2011 Underwater components of humpback whale bubble-net feeding behaviour. *Behaviour* **148**, 575-602.

4. Baumgartner MF, Mayo CA, Kenney RD. 2007 Enormous carnivores, microscopic food, and a restaurant that's hard to find. In *The urban whale: North Atlantic right whales at the crossroads* (eds. SD Kraus, RM Rolland), pp. 138-171. Cambridge, MA: Harvard University Press.

5. Baumgartner MF, Mate BR. 2003 Summertime foraging ecology of North Atlantic right whales. *Mar. Ecol. Progr. Ser.* **264**, 123-135.

6. Wishner KF, Schoenherr JR, Beardsley R, Chen C. 1995 Abundance, distribution and population structure of the copepod *Calanus finmarchicus* in a springtime right whale feeding area in the southwestern Gulf of Maine. *Continental Shelf Res.* **15**, 475-507.

7. Baumgartner MF, Lysiak NSJ, Schuman C, Urban-Rich J, Wenzel FW. 2011 Diel vertical migration behavior of *Calanus finmarchicus* and its influence on right and sei whale occurrence. *Mar. Ecol. Progr. Ser.* **423**, 167-184.

8. Kraus SD, Rolland RM. 2007 *The urban whale: North Atlantic right whales at the crossroads*. Cambridge, MA: Harvard University Press.

9. Beamish P. 1978 Evidence that a captive humpback whale (*Megaptera novaeangliae*) does not use sonar. *Deep-Sea Res.* **25**, 469-472.

10. McFarland WN. 1971 Cetacean visual pigments. Vision Res. 11, 1065-1076.

11. Meredith RW, Gatesy J, Emerling CA, York VM, Springer MS. 2013 Rod monochromacy and the coevolution of cetacean retinal opsins. *PLoS Genetics* **9**, e1003432.

12. Peichl L, Bermann G, Kröger R. 2001 For whales and seals the ocean is not blue: a visual pigment loss in marine mammals. *Eur. J. Neurosci.* **12**, 1520-1528.

13. Levenson DH, Dizon A. 2003 Genetic evidence for the ancestral loss of short-wavelength-sensitive cone pigments in mysticete and odontocete cetaceans. *Proc. R. Soc. Lond. B* **270**, 673-679.

14. Schweikert LE, Fasick JI, Grace MS. 2016 Evolutionary loss of cone photoreception in balaenid whales reveals circuit stability in the mammalian retina. *J. Comp. Neurol.* **524**, 2873-2885.

15. Fasick JI, Bischoff N, Brennan S, Velasquez S, Andrade G. 2011 Estimated absorbance spectra of the visual pigments of the North Atlantic right whale (*Eubalaena glacialis*). *Mar. Mammal. Sci.* **27**, E321-E-331.

16. Bischoff N, Nickle B, Cronin TW, Velasquez S, Fasick JI. 2012 Deep-sea and pelagic rod visual pigments identified in the mysticete whales. *Visual Neurosci.* **29**, 95-103.

17. Fasick JI, Robinson PR. 2000 Spectral-tuning mechanisms of marine mammal rhodopsins and correlations with foraging depth. *Visual Neurosci.* **17**, 781-788.

18. Land MF. 1981 Optics and vision in invertebrates. In *Handbook of sensory physiology, vol. 7/6B. Vision in invertebrates. Invertebrate visual centers and behavior I* (ed. H Autrum), pp. 471-592. Berlin: Springer-Verlag.

19. Land MF, Nilsson D-E. 2012 *Animal eyes (2nd edition).* Oxford, UK: Oxford University Press.

20. Buono MR, Fernández MS, Herrera Y. 2012 Morphology of the eye of the southern right whales (*Eubalaena australis*). *Anat. Record* **295**, 355-368.

21. Zhu Q, Hillmann DJ, Henk WG. 2001 Morphology of the eye and surrounding structures of the bowhead whale, *Balaena mysticetus*. *Mar. Mammal Sci.* **17**, 729-750.

22. Johnsen S, Sosik HM. 2003 Cryptic coloration and mirrored sides as camouflage strategies in near-surface pelagic habitats: Implications for foraging and predator avoidance. *Limnol. Oceanogr.* **48**, 1277-1288.

23. Rodieck RW. 1998 The first steps in seeing. Sunderland, MA: Sinauer Associates, Inc.

24. Govardovskii VI, Fyhrquist N, Reuter T, Kuzmin DG, Donner K. 2000 In search of the visual pigment template. *Visual Neurosci.* **17**, 509-528.

25. Cronin TW, Johnsen S, Marshall NJ, Warrant EJ. 2014 *Visual ecology*. Princeton, NJ: Princeton University Press.

26. Jerlov NG. 1976 *Marine optics*. New York: Elsevier.

27. Aho A-C, Donner K, Helenius S, Larsen LO, Reuter T. 1993 Visual performance of the toad (*Bufo bufo*) at low light levels: retinal ganglion cell responses and prey-catching accuracy. *J. Comp. Physiol. A* **172**, 671-682.

28. Warrant E. 2004 Vision in the dimmest habitats on earth. *J. Comp. Physiol. A* **190**, 765-789.

29. Nilsson D-E, Warrant E, and Johnsen S. 2014 Computational visual ecology in the pelagic realm. *Phil. Trans. Roy. Soc. B* **369**, 20130038.

30. Cronin TW, Goldsmith TH. 1982 Quantum efficiency and photosensitivity of the rhodopsin-metarhodopsin conversion in crayfish photoreceptors. *Photochem. Photobiol.* **36**, 447-454.

31. Supin AY, Popov VV, Mass AM. 2001 *The sensory physiology of aquatic mammals.* Boston: Kluwer Academic Publishers.

32. Reuter T, Peichl L. 2008 Structure and function of the retina in aquatic tetrapods. In *Sensory evolution on the threshold – adaptations in secondarily aquatic* vertebrates (eds. JGM Thewissen, S Numella), pp. 149-172. Berkeley, University of California Press.

33. Warrant EJ. 1999 Seeing better at night: life style, eye design and the optimum strategy of spatial and temporal summation. *Vision Res.* **39**, 1611-1630.

34. Murayama T, Somiya H, Aoki I, Ishii T. 1992 The distribution of ganglion cells in the retina and visual acuity of minke whale. *Nippon Suisan Gakkaishi* **58**, 1057-1061.

35. Mass AM, Supin AY. 1997 Ocular anatomy, retinal ganglion cell distribution, and visual resolution in the gray whale, *Eschrichtius gibbosus. Aquatic Mammals* ***23*****.1**, 17-28.

36. Silveira LCL, Saito CA, Lee BB, Kremers J, Filho MS, Kilavik BE, Yamada ES, Perry VH. 2004 Morphology and physiology of primate M- and P-cells. *Progr. Brain Res.* **144**, 21-46.

37. Gagnon YL, Shashar N, Warrant EJ, Johnsen SJ. 2007 Light scattering by selected zooplankton from the Gulf of Aqaba. *J. Exp. Biol.* **210**, 3738-3735.

38. Calambokidis H, Schorr GS, Steiger GH, Francis J, Bakhtiari M, Marshal G, Oleson EM, Gendron D, Robertson K. 2007 Insights into the underwater diving, feeding, and calling behavior of blue whales from a suction-cup-attached video-imaging tag (Crittercam*). Mar. Technol. Soc. J.* **41**, 19-29.

39. Levenson DH, Schusterman RJ. 1999 Dark adaptation and visual sensitivity in shallow and deep-diving pinnipeds. *Mar. Mammal Sci.* **15**, 1303-1313.

40. Dawson WW, Adams CK, Barris MC, Litzkow CA. 1979 Static and kinetic properties of the dolphin pupil. *Am. J. Physiol.* **6**, R301-R305.

41. Thewissen JGM, George J, Rosa C, Kishida T. 2010 Olfaction and brain size in the bowhead whale (*Balaena mysticetus*). *Mar. Mammal Sci.* **27**, 282-294.

42. Kishida T, Thewissen JGM, Hayakawa T, Imai H, Agata K. 2015 Aquatic adaptation and the evolution of smell and taste in whales. *Zool. Lett.* **1**, 9.

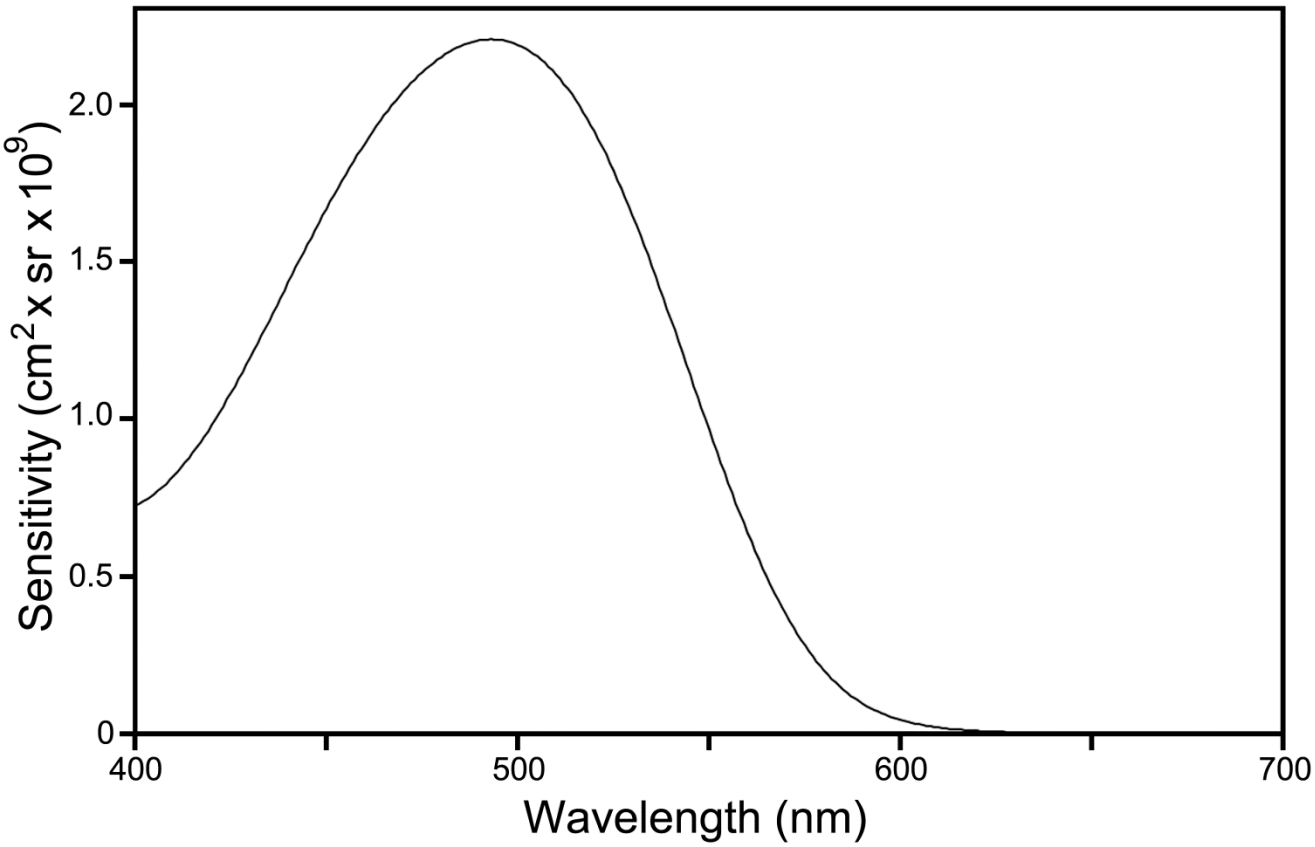

Figure 1. Optical sensitivity spectrum of one *Eubalena glacialis* rod photoreceptor. This curve is calculated using the sensitivity of the eye of *E. australis* (table S1) multiplied by the absorptance spectrum of *E. glacialis* rod photopigment (λ_{max} = 493 nm) from [16], assuming a rod length of 30 µm and a peak absorbance of 0.015 μm^{-1}. See text for details.

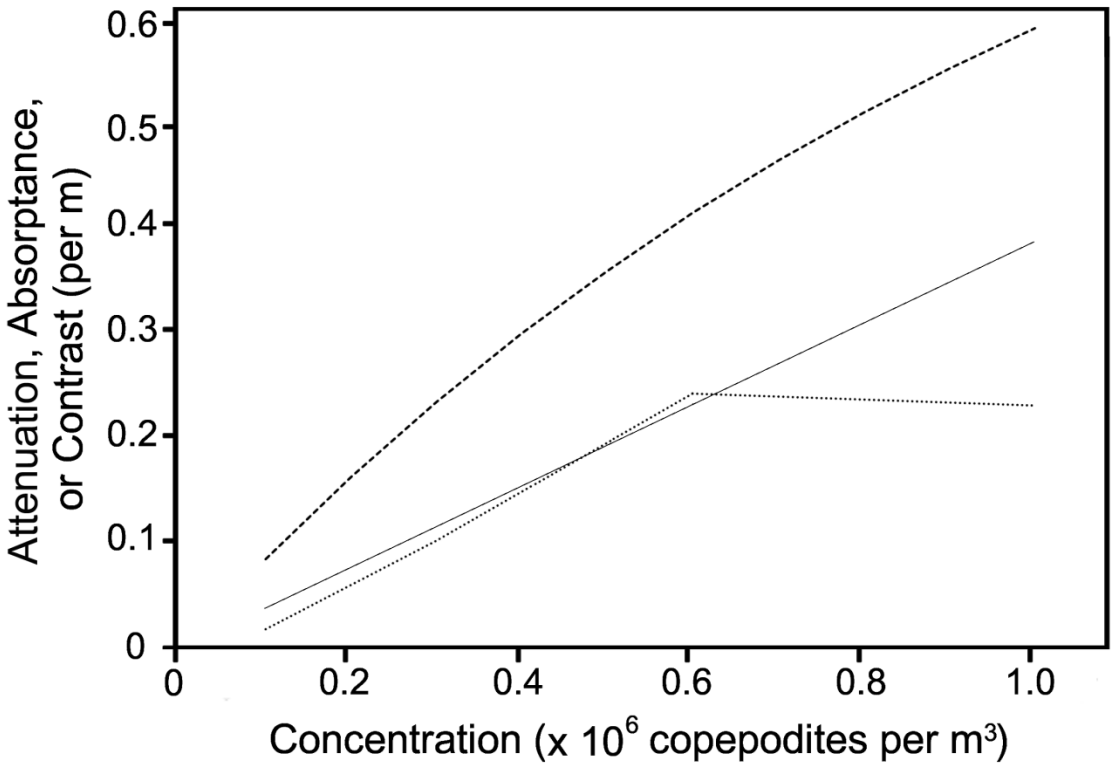

Figure 2. Light absorption and visual contrast of living 5th copepodites of *Calanus finmarchicus* in seawater. Dotted curve: attenuation vs. concentration (averages of the attenuation spectra figure S1). Thin straight line: linear fit to average concentration data (through a concentration of 0.6 copepodites m^{-3}) forced to pass through the origin y = 0.0386x. Dashed curve: absorptance (proportion of light removed) corresponding to the fitted curve, which is identical to the Weber contrast of copepod patches viewed at very short distances over this range of concentrations.

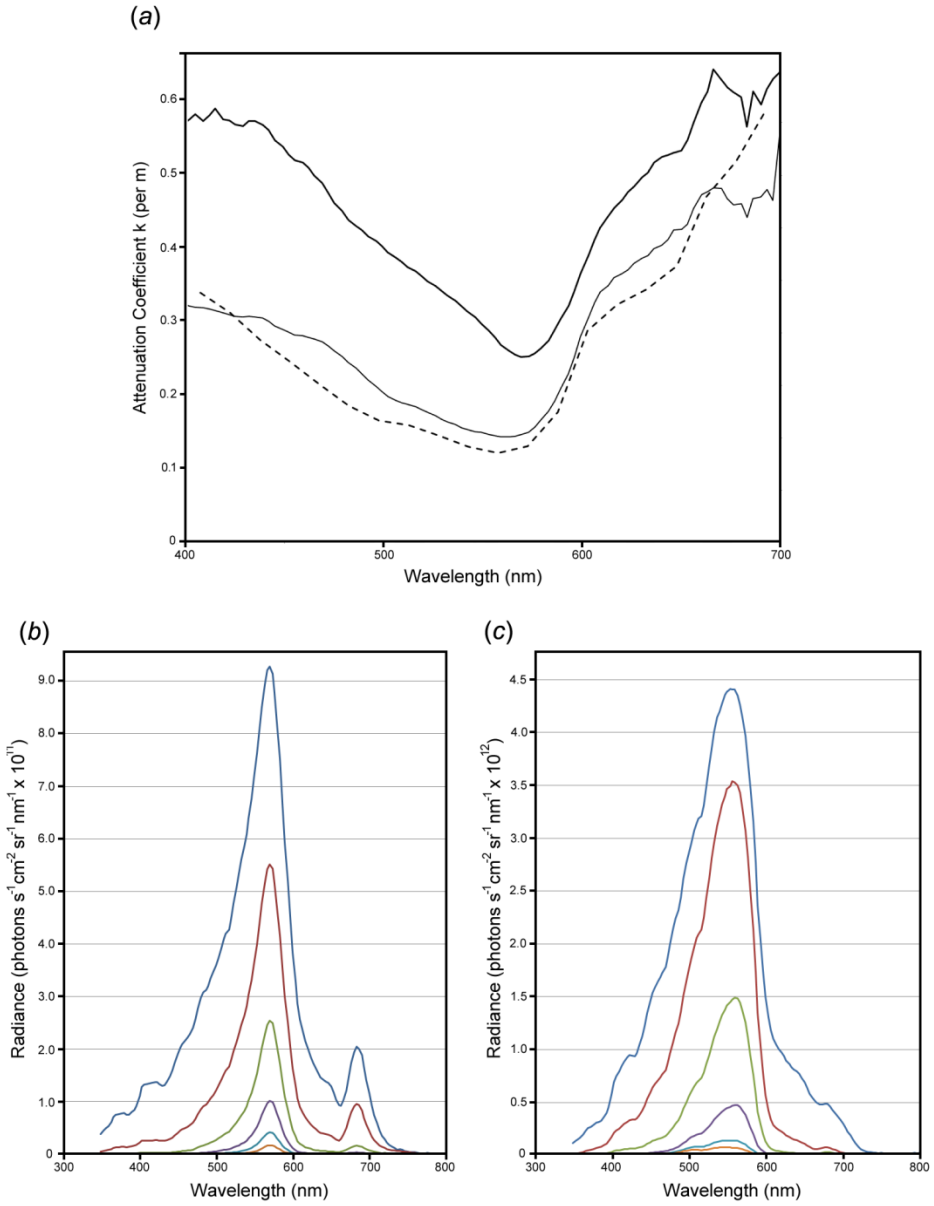

Figure 3. Photic properties of waters where *E. glacialis* feeds. (*a*) Thin solid curve: diffuse attenuation coefficients for the clearest water measured (Great South Channel, May 8, 2013). Thick solid curve: diffuse attenuation spectrum of the least clear water measured (Wilkinson Basin, April 4, 2012). Dashed curve: diffuse attenuation spectrum of waters off Portsmouth, New Hampshire (June 30, 2000) measured in [22]. (*b*) Horizontal radiance spectra from Wilkinson Basin series averaged over 4-m depth ranges plotted for center depths of 2, 6, 10, 14, 18, and 22 m. (*c*) Horizontal radiance spectra from the Great South Channel series averaged over 4-m depth ranges plotted for center depths of 2, 6, 10, 14, 18, and 22 m.

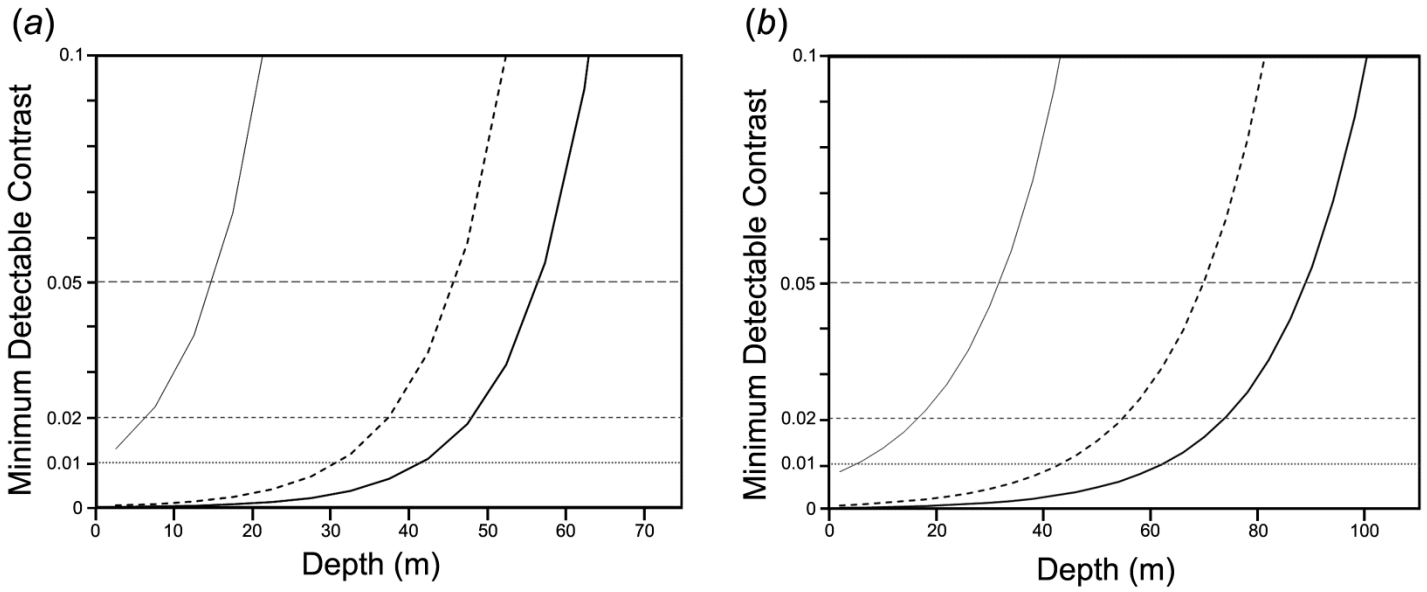

Figure 4. Calculated minimum detectable contrast for extended objects viewed horizontally at ~0 m range vs. depth for *E. glacialis* in (*a*) the most turbid waters we measured (Wilkinson Bay) and (*b*) the clearest waters we measured (Great South Channel). In both panels, thin solid lines plot trended data (based on photon absorption rates from trends in figure S2) for contrast detectable by single rods; dashed curves are calculated from trended data for pools of 100 rods; and thick solid curves are calculated from trended data for pools of 1000 rods. Horizontal lines show minimum detectable contrasts for thresholds of 0.05, 0.02, and 0.01. Portions of the curve that are below each horizontal line correspond to depths at which there is sufficient light to view contrasts at or above the corresponding threshold.

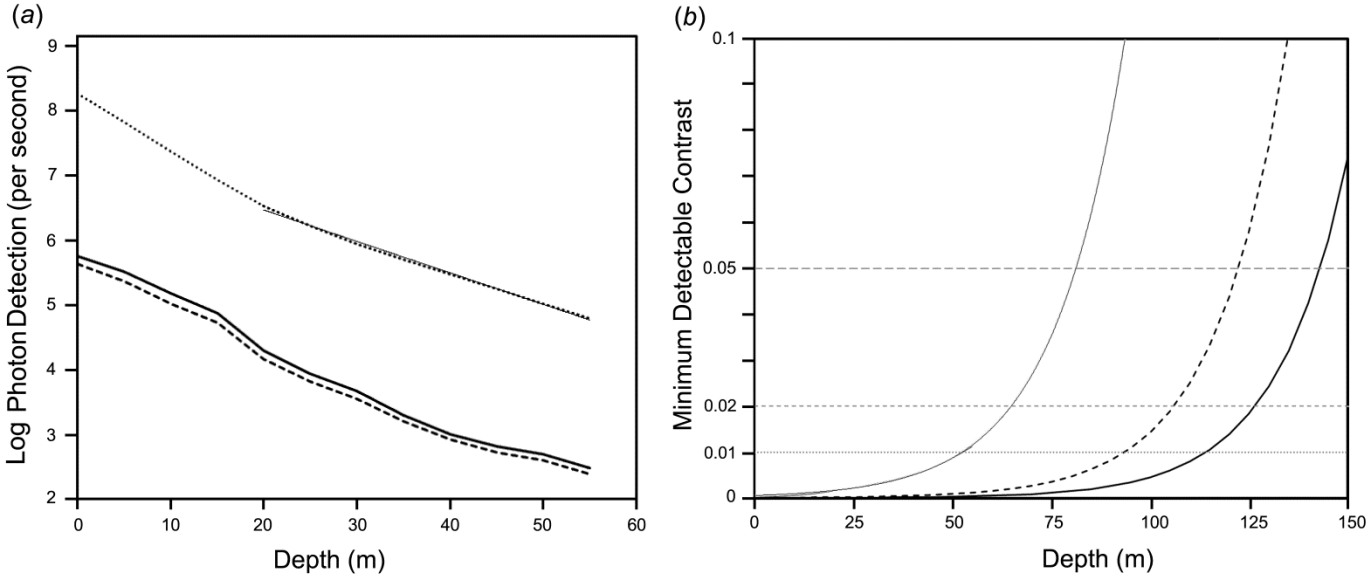

Figure 5. (*a*) Calculated log photon detection for *E. glacialis* rods in waters off Portsmouth, New Hampshire [22]. Dark solid curve: horizontal viewing away from the sun's azimuth. Dark dashed curve: horizontal viewing towards the sun's azimuth. Dotted curve: vertical viewing, looking upward (the thin straight line shows the log-linear fit to the data at depths below 20 m, used to compute contrasts plotted in (*b*); $y = 27{,}400{,}000\, e^{-0.0112x}$). (*b*) Calculated minimum detectable contrast for extended objects viewed vertically vs. depth for *E. glacialis* looking vertically upward in the conditions illustrated in (*a*). Thin solid curve is calculated using trended data (photon catch rates given by the fit in (*a*)) for contrast detectable by single rods; dashed curve is calculated from trended data for pools of 100 rods; and thick solid curve is calculated from trended data for pools of 1000 rods. Horizontal lines show minimum detectable contrasts at thresholds of 0.05, 0.02, and 0.01; portions of the curve that are below each horizontal line correspond to depths at which there is sufficient light to view contrasts at or above the corresponding threshold.